

# Intensity-Dependent Adaptation of Cortical and Thalamic Neurons Is Controlled by Brainstem Circuits of the Sensory Pathway

Elad Ganmor,<sup>1</sup> Yonatan Katz,<sup>1</sup> and Ilan Lampl<sup>1,\*</sup>

<sup>1</sup>Department of Neurobiology, Weizmann Institute of Science, Rehovot 76100, Israel

\*Correspondence: ilan.lampl@weizmann.ac.il

DOI 10.1016/j.neuron.2010.03.032

## SUMMARY

Current views of sensory adaptation in the rat somatosensory system suggest that it results mainly from short-term synaptic depression. Experimental and theoretical studies predict that increasing the intensity of sensory stimulation, followed by an increase in firing probability at early sensory stages, is expected to attenuate the response at later stages disproportionately more than weaker stimuli, due to greater depletion of synaptic resources and the relatively slow recovery process. This may lead to coding ambiguity of stimulus intensity during adaptation. In contrast, we found that increasing the intensity of repetitive whisker stimulation entails less adaptation in cortical neurons. In a series of recordings, from the trigeminal ganglion to the thalamus, we pinpointed the source of the unexpected pattern of adaptation to the brainstem trigeminal complex. We suggest that low-level sensory processing counterbalances later effects of short-term synaptic depression by increasing the throughput of high-intensity sensory inputs

## INTRODUCTION

In all sensory modalities, elevation in stimulation intensity usually causes a transient increase in firing rate followed by a slow decline toward a lower level. The functional role of this adaptation process is not clear, but it has been hypothesized to serve several different roles (Wark et al., 2007). Adaptation alters the sensitivity of neuronal circuits to match the prevailing conditions in order to efficiently encode sensory stimuli (Adorján et al., 1999; Brenner et al., 2000; Fairhall et al., 2001; Maravall et al., 2007; Müller et al., 1999; Sharpee et al., 2006). Adaptation may also improve the detectability of rare stimuli by suppressing responses to frequent stimuli while enhancing or leaving responses to novel stimuli unchanged (Dragoi et al., 2002; Ulanovsky et al., 2003). Other studies have hypothesized that adaptation mediates predictive coding (Lundstrom et al., 2008), enabling neural responses to precede temporally correlated sensory inputs.

Several neural mechanisms are involved in sensory adaptation (Kohn, 2007), including intrinsic (Carandini and Ferster, 1997;

Díaz-Quesada and Maravall, 2008; Sanchez-Vives et al., 2000a, 2000b) and inhibitory mechanisms (Barlow, 1990; Carvalho and Buonomano, 2009; Chelaru and Dragoi, 2008; Wainwright et al., 2002). Synaptic depression in particular has been suggested to play a major role in adaptation of sensory inputs in different modalities, including the visual (Chance et al., 1998), auditory (Wehr and Zador, 2005), and somatosensory (Chung et al., 2002; Heiss et al., 2008; Katz et al., 2006; Khatri et al., 2004) systems (for review see Zucker and Regehr, 2002).

In the rat somatosensory system, stimuli delivered to the facial vibrissae are conveyed to layer 4 of the primary somatosensory cortex via three synapses (Petersen, 2003) and through at least four parallel pathways (Urbain and Deschênes, 2007; Yu et al., 2006). The lemniscal pathway, which provides powerful short latency input to the primary somatosensory cortex, originates in afferent fibers that innervate whisker follicles and synapse onto neurons in the principalis nucleus of the brainstem trigeminal complex (PrV). These PrV neurons send axons to the ventral posterior medial nucleus of the thalamus (VPM), which in turn delivers sensory input to layer 4 cortical cells. Several studies suggested a major role for synaptic depression in layer 4 adaptation (Chung et al., 2002; Gabernet et al., 2005; Heiss et al., 2008; Katz et al., 2006; Khatri et al., 2004). Less is known about adaptation at earlier stages of the somatosensory system, although studies of VPM also suggest a role for synaptic depression in thalamic adaptation (Castro-Alamancos, 2002b; Deschênes et al., 2003).

Studies of short-term synaptic depression led to highly successful mathematical descriptions of this phenomenon (Tsodyks and Markram, 1997). Assuming adaptation in the lemniscal pathway results mostly from synaptic depression gives rise to several interesting predictions. First, these models predict that an increase in stimulus intensity, which is followed by higher firing probability at early sensory stages, will raise the effective frequency of stimulation, resulting in greater depression during repetitive stimulation due to depletion of synaptic resources and the relatively slow recovery processes (see Figure 1A and Supplemental Experimental Procedures for details). In addition, during adaptation, responses to low-intensity stimuli may actually surpass those to higher-intensity stimuli. This may prevent the decoding of stimulus intensity from response magnitude, leading to coding ambiguity during adaptation (Figure 1B).

We tested these hypotheses in vivo, in cortical, thalamic, brainstem, and first-order sensory stages and found that our results do not agree with the predictions of short-term synaptic

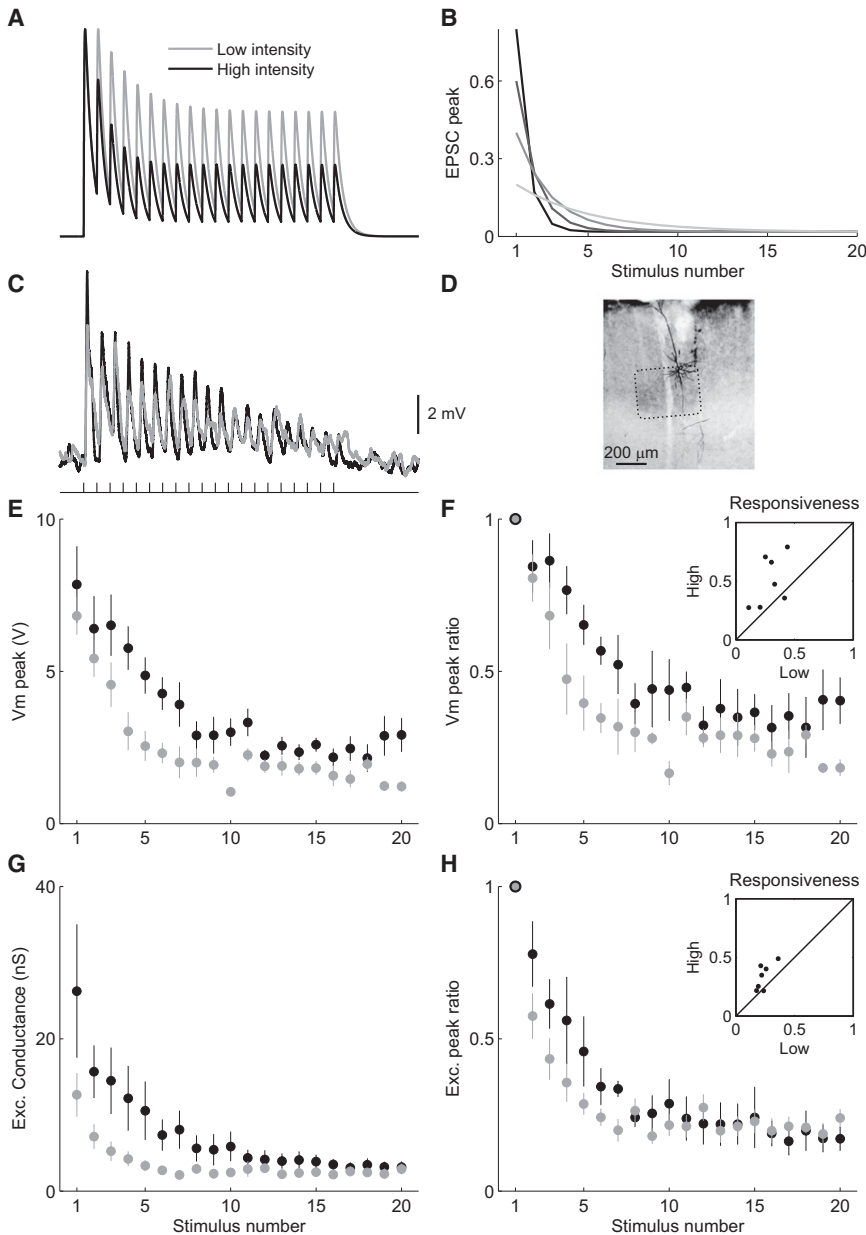


**Figure 1. Cortical Adaptation to Different Stimulus Intensities Does Not Follow Models of Short-Term Synaptic Depression**

(A) Simulated membrane potential of a model neuron receiving repetitive input through a classic depressing synapse (see **Experimental Procedures**), 18 Hz stimulus train shown below bottom trace. High-intensity stimulation (black) is modeled by high probability of presynaptic firing, while low intensity (gray) is associated with a lower firing probability. The synaptic response decays less in the low-intensity condition.

(B) Theoretical adaptation curves based on short-term synaptic depression (see **Experimental Procedures** for details). Curves show response magnitude to repetitive stimulation given different presynaptic firing probabilities (darker color denotes greater probability; arbitrary units). Notice that after the second stimulus the curves intersect, leading to possible coding ambiguity.

(C) Intracellular recording of a cortical neuron that receives direct thalamic input. The average membrane potential in response to high-intensity (black) and low-intensity stimulation (gray) is shown. Stimulus delivery times are denoted below the trace.

(D) Reconstruction of the neuron in (B). Dashed line marks borders of the layer 4 barrel.

(E) Population ( $n = 7$ ) EPSP peak is plotted as a function of stimulus number (bars represent SEM).

(F) Population voltage peak adaptation ratio. Actual voltage peak is divided by peak EPSP evoked by the first stimulus to produce the ratio (bars represent SEM). (Inset) Responsiveness index (F1, see **Supplemental Experimental Procedures**) of the voltage response in the high-intensity condition (ordinate) is plotted against the value calculated for the low-intensity condition (abscissa). In six out of seven cells, a greater responsiveness index (i.e., less adaptation) was measured in the high-intensity condition.

(G and H) Same as (E) and (F), but for the peak estimated excitatory conductance. Clearly, in contrast to the prediction of the model, the response to the low-intensity stimulus does not decay less than the response to the high-intensity stimulus.

depression models, suggesting that other mechanisms act to counterbalance the effects of synaptic depression in early sensory processing.

## RESULTS

### Cortical Adaptation to Stimuli of Different Intensities Does Not Follow Short-Term Synaptic Depression Models

Models of short-term synaptic depression predict that increasing stimulation intensity will result in greater response adaptation, which may lead to ambiguity in the coding of stimulus intensity during adaptation (Figures 1A and 1B; see **Introduction** for more details). We tested this hypothesis in the rat barrel

cortex, whose inputs are thought to adapt mainly due to short-term synaptic depression. To that end, we applied repetitive whisker stimulation at frequencies within the natural whisking range when performing object discrimination tasks (Berg and Kleinfeld, 2003) (18 Hz, 20 stimuli). Stimuli were delivered at two very different intensities while recording intracellularly from cortical cells located within or having dendritic innervations in layer 4 and presumably receive direct thalamic input ( $n = 7$ ; see Figures 1C and 1D for example neuron). The high-intensity stimulation was set to the maximal deflection of the stimulator, and the weak stimulation was selected online such that it evoked a significantly smaller response. The exact amplitude and velocity of the weak stimulation was different across the population, since a sharp drop in response probability was

observed at very different stimulation intensities. This could be due to the fact that different whiskers were used in this study and the different angular tuning properties of the recorded neurons (Andermann and Moore, 2006; Kerr et al., 2007). Across all recordings, we verified that the response probability evoked by the first stimulus for the weak stimulation was at least 10% smaller than for the strong stimulus.

Adaptation of cortical cells was quantified by the peak average subthreshold response for each stimulus divided by the peak of the first response, providing a peak response adaptation ratio (Figure 1F). We also calculated the F1 index (responsiveness index; see Supplemental Experimental Procedures), which measures the ratio of the power at the stimulation frequency of the recorded response and that of an ideal nonadapted response (<1 corresponding to adaptation, >1 corresponding to facilitation; Figure 1F, inset).

In contrast to the short-term synaptic depression model, we found that not only does the voltage response to high-intensity stimulus not adapt more than in the low-intensity condition, it actually adapts slightly less than the response to weaker stimulation (Figures 1E and 1F). In six out of seven cells, the F1 index of the response to high-intensity stimulus was higher than that to low-intensity stimulus ( $p < 0.02$ , one-sided two-sample Wilcoxon signed-rank test). Importantly, at these stimulation conditions, we observe no intersection of the response curves, as may occur theoretically (Figure 1B), avoiding possible coding ambiguity and allowing for stimulus intensity to be decoded from response magnitude even during adaptation.

However, the amplitude of the voltage response can be affected by inhibition (Heiss et al., 2008; Moore and Nelson, 1998), which may mask the actual adaptation of the excitatory input to the cell. To overcome this, we used conductance estimates (see Experimental Procedures). When considering only the estimated excitatory inputs to these cells, we found similar results (Figures 1G and 1H), suggesting that the excitatory input to cortical cells that presumably receive direct thalamic input adapts less in response to high-intensity stimuli than in the case of low-intensity stimuli.

The above results indicate that our initial hypothesis does not hold in layer 4 of the primary somatosensory cortex, and thus sensory adaptation cannot be fully explained by short-term plasticity models. This intriguing outcome led us to seek the source of this phenomenon subcortically.

### Recordings of First-Order Sensory Neurons Do Not Provide an Explanation to Intensity-Dependent Cortical Adaptation

Could our observations in the cortex be explained at the first stage of neuronal encoding of whisker mechanical movements? To examine this possibility, we measured the peripheral firing responses to whisker stimulation prior to the recruitment of any synapses.

We recorded the responses of single units in the trigeminal ganglion (TG,  $n = 13$ ). These neurons are the first-order sensory neurons in the vibrissal pathway and innervate the whisker follicles directly. Although TG neurons respond with high temporal precision (Arabzadeh et al., 2006; Gottschaldt and Vahle-Hinz, 1981; Jones et al., 2004; Shoykhet et al., 2000), we verified

that arbitrary choice of bin size does not affect our results by quantifying adaptation at the two extremes of temporal precision. On the one hand, we measured the ratio of the population PSTH peak response to each stimulus in the train and that of the first stimulus at 1 ms accuracy, which is approximately the jitter of single responses (peak response adaptation ratio, Figure 2B). On the other hand, we compared the total number of spikes evoked by each stimulus to that evoked by the first stimulus, regardless of exact spike timing (spike count adaptation ratio; Figure 2D). The population PSTH is commonly used as an estimate for the input to downstream layers (Sarid et al., 2007); therefore, these measures serve as a proxy for the input to downstream sensory processing stations.

These data verify that stronger stimuli result in higher firing probability (Figure 2A) and a greater number of spikes per stimulus (Figure 2C). We found that responses of TG cells to repetitive stimulation adapt much less than cortical responses. Since no synapses are involved in the sensory processing at the TG stage, we expect no difference in the adaptation patterns evoked by the two stimulus conditions. The peak response adaptation ratio pointed toward slightly less adaptation for the weak stimulation (Figure 2B). This difference proved statistically significant when comparing the steady-state response (taken to be the average response to the last five stimuli) in the two conditions ( $p < 0.01$ ,  $n = 13$ , two-sided two-sample Wilcoxon signed-rank test). The spike count adaptation ratio showed no difference between the two conditions (Figure 2D).

Since more spikes are evoked per whisker deflection by the high-intensity stimulus and given that no major difference was found in the adaptation pattern for the two intensities, neurons downstream to the trigeminal nucleus should adapt more in response to high-intensity stimulation, due to synaptic depression.

### VPM Neurons Adapt Less in Response to High-Intensity Stimuli

The lack of adaptation in first-order TG cells and the clear discrepancy between the predictions of the classical short-term synaptic plasticity model and the adaptation patterns observed in cortex led us to investigate the direct feed-forward thalamic input to cortical layer 4 in order to shed light on the source of these unexpected adaptation patterns.

Previous studies showed that the VPM provides the major subcortical input to layer 4 cells in the barrel cortex (Bruno and Sakmann, 2006; Gil et al., 1999; Pierret et al., 2000). Similar to the cortex, adaptation of VPM responses is believed to result from synaptic depression (Deschênes et al., 2003). Therefore, as previously explained, we expected that thalamic cells will adapt more in response to high-intensity stimulation, compared to the low-intensity condition.

Using high-impedance glass electrodes (see Experimental Procedures), we recorded extracellularly the spikes of single VPM neurons responding to strong and weak repetitive stimulation ( $n = 32$ ). Clearly, and even more pronounced than in cortex, the responses to high-intensity stimulation adapted significantly less than the responses in the low-intensity condition (Figures 3A–3D,  $p < 10^{-10}$  for the steady-state response of both PSTH peak and spike-count ratio, one-sided two-sample Wilcoxon

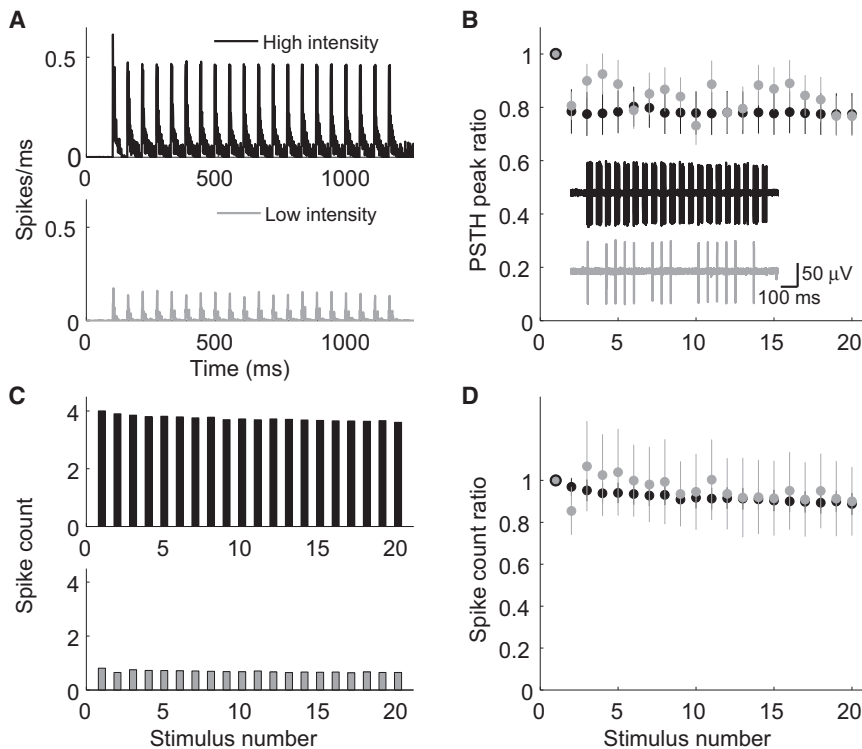


**Figure 2. Adaptation of First-Order Sensory Neurons in the TG Is Negligible and Is Not Intensity Dependent**

(A) TG population ( $n = 13$ ) PSTH of responses to repetitive whisker stimulation at 18 Hz for both stimulus conditions.

(B) Average PSTH peak response adaptation ratio is plotted against stimulus number (time bin of 1 ms, bars represent SEM). Actual PSTH peak values are divided by the peak of the first response to produce the ratio. (Inset) Example traces of a TG neuron's response to both stimulus conditions (Top: high intensity, black. Bottom: Low intensity, gray).

(C) Population average of the number of spikes evoked per stimulus (55 ms bins) is plotted against stimulus number, for both intensities.

(D) Average spike count adaptation ratio is plotted against stimulus number (bars represent SEM). Actual spike counts are divided by the number of spikes evoked by the first stimulus to produce the ratio. TG neurons adapt very little compared to cortex and display little intensity-dependent adaptation.

signed-rank test). Considering the sensory responses of TG neurons, these results seem to contradict the assumption that adaptation of VPM responses is purely a result of synaptic depression.

### Timescales of Intensity-Dependent Adaptation

Intensity-dependent adaptation may result from rapid feed-forward mechanisms that control the gain of the adaptation process instantaneously, or it may involve much slower timescales. To test this, we applied a recovery protocol to a subset of recorded thalamic cells ( $n = 7$ ). As before, we delivered a train of 20 stimuli at 18 Hz, but in addition we delivered a test stimulus of the same intensity as the train, 1, 2.3, or 5 s after the end of the train (Figure 4A). Recovery was quantified in a similar way to adaptation, by measuring either the ratio of the PSTH peak or the spike count for the test response and the first response. Similarly to high-frequency stimulus trains, the test responses to high-intensity stimuli exhibited significantly better recovery (i.e., less adaptation) on timescales of up to 5 s. Responses to high-intensity stimuli fully recovered and even facilitated after 1 s (peak recovery ratio  $1.11 \pm 0.16$ ), whereas responses to low-intensity stimuli remained significantly depressed even after 5 s (peak recovery ratio  $0.84 \pm 0.08$ ,  $p < 0.01$ , one-sided one-sample Wilcoxon signed-rank test,  $n = 7$ ). Significant differences between the two conditions were evident at all timescales for the peak recovery ratio (Figure 4B) and after 1 s in the spike-count recovery ratio as well (Figure 4C,  $p < 0.05$ , one-sided two-sample Wilcoxon signed-rank test,  $n = 7$ ).

Slow recovery from stimulus trains and adaptation to high-frequency stimulation display the same dependency on stimulus

intensity: low-intensity stimuli adapt more and recover more slowly. This suggests that these two phenomena may share common mechanisms with slow kinetic components, on time-scales of seconds.

### The Role of Feedback Inhibition in the Thalamus

Neurons in the reticular thalamic nucleus (RT) receive excitatory input from the VPM and cortex, and in turn, send feedback inhibition to the VPM. The RT constitutes the only known source of inhibitory input to VPM cells (Pinault, 2004; Shosaku et al., 1989). Previous studies report that RT responses adapt much more than thalamic responses in response to high-frequency repetitive stimulation (Hartings et al., 2003; Yu et al., 2009). It is possible therefore that reduced firing of RT neurons due to adaptation during repetitive stimulation may disinhibit the VPM, causing a recovery of VPM responses and thus may explain the unexpected adaptation pattern of thalamic cells. Simultaneous paired whisker-aligned recordings of VPM single units and multiunit activity in the RT ( $n = 5$ ) supported this conjecture. We observed that while VPM responses exhibit some recovery after about the tenth stimulus, RT responses recover much less, if at all (Figure 5A). We therefore speculated that RT responses to high-intensity stimuli will depress more profoundly than the responses to low-intensity stimuli and thus disinhibit the VPM, resulting in less adaptation to stronger stimuli.

Though RT neurons receive input from the VPM, adaptation of multiunit activity in the RT ( $n = 11$ ) did not display the same dependence on stimulus intensity observed in the VPM. The PSTH peak response adaptation ratio was smaller for the steady-state response to the high-intensity stimulus (Figures

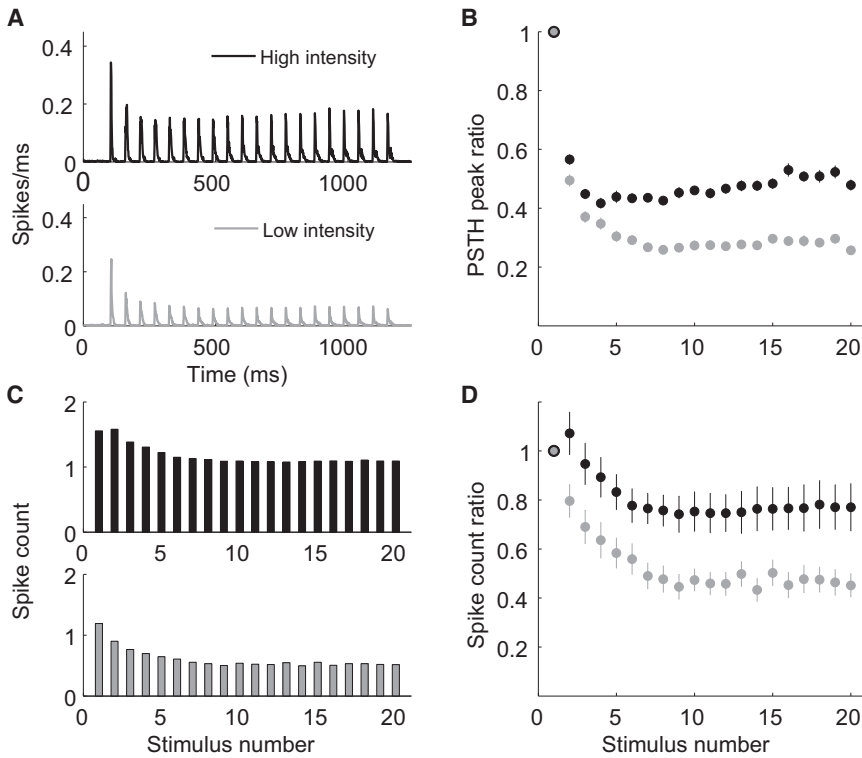


**Figure 3. VPM Neurons Display Disproportionately Greater Adaptation with Reduced Stimulus Intensity, in Contrast to Short-Term Synaptic Depression Behavior**

(A) VPM population ( $n = 32$ ) PSTH of responses to repetitive whisker stimulation at 18 Hz to both stimulus conditions.

(B) Average PSTH peak response adaptation ratio is plotted against stimulus number (bars represent SEM). Actual PSTH peak values are divided by the peak of the first response to produce the ratio.

(C) Population average of the number of spikes evoked per stimulus (55 ms bins) is plotted against stimulus number, for both intensity conditions.

(D) Average spike count adaptation ratio is plotted against stimulus number (bars represent SEM). Actual spike counts are divided by the number of spikes evoked by the first stimulus to produce the ratio. Adaptation of VPM neurons is clearly intensity dependent. Response to low-intensity stimuli adapt more than responses to high-intensity stimuli.

5C and 5D  $p < 10^{-10}$ ,  $n = 11$ , one-sided two-sample Wilcoxon signed-rank test), indicating greater adaptation to the stronger stimulus, as predicted by our initial hypothesis, while the spike-count adaptation ratio showed no significant difference between the two conditions (Figures 5E and 5F). This result can, in theory, provide an explanation to our surprising observations in VPM and cortex, but it is not sufficient to conclude that feedback inhibition is the cause.

### Intracellular Recordings of VPM Neurons Indicate Involvement of Brainstem Mechanisms in Intensity-Dependent Adaptation of Thalamic and Cortical Cells

Our next goal was to examine if indeed thalamic feed-back mechanisms are the cause of the intensity-dependent adaptation we observed, or whether it is a property of feed-forward inputs from the brainstem. One approach would be to somehow manipulate or block inhibition (Castro-Alamancos, 2002a; Cotillon-Williams et al., 2008), but this runs the risk of inadvertently affecting network behavior. To address this question, we proceeded by performing intracellular recordings of VPM neurons.

Using sharp electrodes, we recorded the membrane potential of VPM neurons responding to both stimulus conditions ( $n = 13$ ). In agreement with previous studies, we observed large EPSPs in our recordings (Figure 6A), which are thought to reflect inputs from few brainstem fibers (Castro-Alamancos, 2002b; Deschênes et al., 2003). Since spontaneous firing rates are low in VPM ( $2.27 \pm 6.01$  Hz) and because evoked and spontaneous spikes are almost always a result of an EPSP (Figure 6B), we considered both spikes and EPSPs observed 3–25 ms poststim-

ulus as synaptic input. Even if any form of feedback mechanism is the cause for failure to generate spikes, then we would still be able to observe trigemino-thalamic EPSPs in the VPM, but they would fail to elicit a spike. An adaptation ratio was constructed by calculating the ratio of the probability of observing synaptic input for each response and that of the first response. Similar to the spiking activity of VPM cells, the probability of synaptic input to VPM cells depresses significantly less in response to high-intensity stimulation compared to low-intensity stimulation, as quantified by the adaptation ratios of the steady-state response (Figure 7C,  $p < 10^{-4}$ , one-sided two-sample Wilcoxon signed-rank test). Note that the probability of observing an EPSP for the first stimulation was higher when high-intensity stimulation was used (inset above Figure 6C). This clearly suggests that the transmission failures and the surprising adaptation patterns they entail originate in the brainstem trigeminal complex.

It is still possible that in addition to reduced probability of brainstem inputs during repetitive whisker stimulation, the size of evoked synaptic potentials is decreased as a result of short-term depression. To measure the size of evoked synaptic inputs, we blocked firing in a subset of cells ( $n = 3$ ) using QX-314 and measured the average EPSP size (only trials in which an EPSP was detected were averaged). Two out of the three cells displayed significantly larger adapted EPSPs in response to the weaker stimulus (Figure 6D; Cell-1: low-intensity EPSP =  $12.2 \pm 2.67$  mV,  $n = 3$ , high-intensity EPSP =  $7.87 \pm 1.40$  mV,  $n = 130$ ,  $p < 0.01$ , Mann-Whitney U test. Cell-2: low-intensity EPSP =  $21.0 \pm 6.12$  mV,  $n = 562$ , high-intensity EPSP =  $16.3 \pm 4.28$  mV,  $n = 2778$ ,  $p < 10^{-10}$ , Mann-Whitney U test), while the third cell showed no significant difference (low-intensity EPSP =  $8.12 \pm 1.32$  mV,  $n = 26$ , high-intensity EPSP =  $8.25 \pm 0.76$  mV,  $n = 16$ ,  $p = 0.5$ , Mann-Whitney U test). These results suggest that the trigemino-thalamic synapse is more depressed in the high-intensity

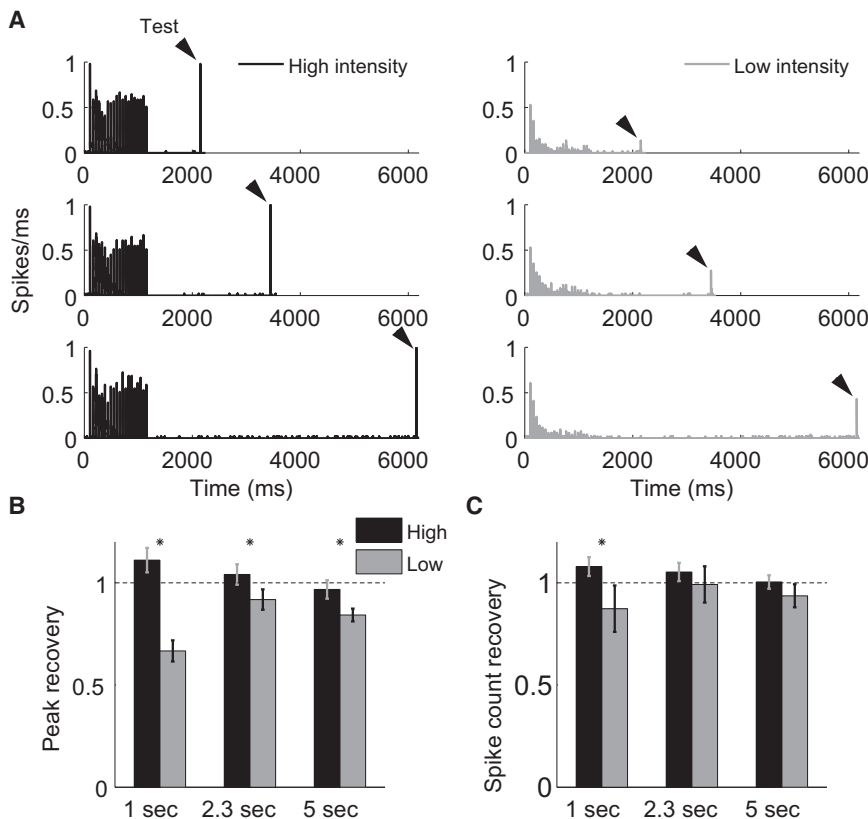


**Figure 4. Recovery from Adaptation in VPM, on a Timescale of Seconds, Is Intensity Dependent**

(A) PSTHs of a VPM neuron responding to an 18 Hz 20 stimulus train, with a test stimulus delivered 1 (top), 2.3 (middle), or 5 (bottom) seconds after the end of the train (marked by arrowhead). Left: high-intensity condition. Right: Low-intensity condition.

(B) Average PSTH peak recovery ratio (peak of the test response divided by that of the first response in the train) after different periods of recovery ( $n = 7$ , error bars denote SEM). While responses to high-intensity stimuli slightly facilitate, weaker stimuli slowly recover from adaptation. Dashed line represents full recovery.

(C) Average recovery ratio of the number of spikes per stimulus (55 ms bin) after different periods of recovery. The number of spikes evoked by the test stimulus was divided by the number of spikes evoked by the first stimulus of the train.

condition, probably due to increased presynaptic firing and more synaptic release events. Hence, the failures in transmission are not a result of synaptic fatigue, but the failure of brainstem neurons to generate spikes. Together with our knowledge of first-order sensory responses, our results point to brainstem circuitry as the source of the adaptation patterns we report here.

### Recordings in PrV Verify that the Locus of the Reported Adaptation Behavior Is the Brainstem

To verify our conclusions from intracellular recordings of VPM neurons, we proceeded to record extracellularly from the PrV. Single and multiunit responses recorded under the same stimulation conditions displayed adaptation patterns similar to those observed in the VPM. Namely, responses to high-intensity stimuli adapted less and recovered faster, both for peak response (Figures 7A and 7B;  $p < 10^{-10}$  for the steady-state response,  $p < 10^{-3}$  for the recovery response, one-sided two-sample Wilcoxon signed-rank test) and for total spike count (Figures 7C and 7D;  $p < 10^{-10}$  for the steady-state response,  $p < 0.05$  for the recovery response, one-sided two-sample Wilcoxon signed-rank test). Because of the diversity of brainstem projections (Veinante and Deschênes, 1999) (see also Discussion), it is hard to prove that the cells we recorded in fact project directly to VPM neurons. However, combined with our intracellular VPM data, these data provide strong evidence that the adaptation pattern we report here originates in the brainstem.

Can the observed data be explained by a simple model with short-term synaptic depression and a nonlinear threshold func-

tion (“iceberg effect,” see Figure S3A for illustration)? According to this plausible explanation, low-intensity stimulation may result in less adaptation (as expected from synaptic depression), yet the adapted responses will be below the neuron’s firing threshold, whereas responses to stronger stimuli adapt proportionally more but remain above threshold, resulting in less firing adaptation for high-intensity stimuli. To test this possibility we fit such a model to the experimental data recorded in the brainstem (Figure 8A; see Supplemental Experimental Procedures and Figure S3A for details). In particular, we asked if the parameters obtained by fitting the adaptation phase of the response can explain the recovery from adaptation. Although this model can explain the early depression phase of the data, namely the responses to the high-frequency train and the greater firing adaptation to weak stimulation, the best model for the depression phase (fit to the 20 responses during the 18 Hz train) clearly fails in predicting the recovery test response occurring 1 s later (Figure 8A). Moreover, fitting simultaneously both the depression phase and recovery response using the same set of parameters was unable to accurately capture the entire data, in particular for the low-intensity stimulus (data not shown).

To further examine the plausibility of the “iceberg effect” in the peculiar pattern of adaptation in the brainstem, local field potential (LFP) was recorded simultaneously with single and multiunit recordings. Little is known about LFP signals in the brainstem, yet based on the latency of evoked LFP and the shape of spontaneous spike-triggered average LFP (Figure S3B), it is likely that the LFP reflects feed-forward synaptic inputs. If the “iceberg effect” were responsible for our observations, then we would expect that LFP adaptation, which is likely to reflect sub-threshold behavior, will be stronger for high-intensity stimulation. We found, however, that the LFP adapted less and recovered

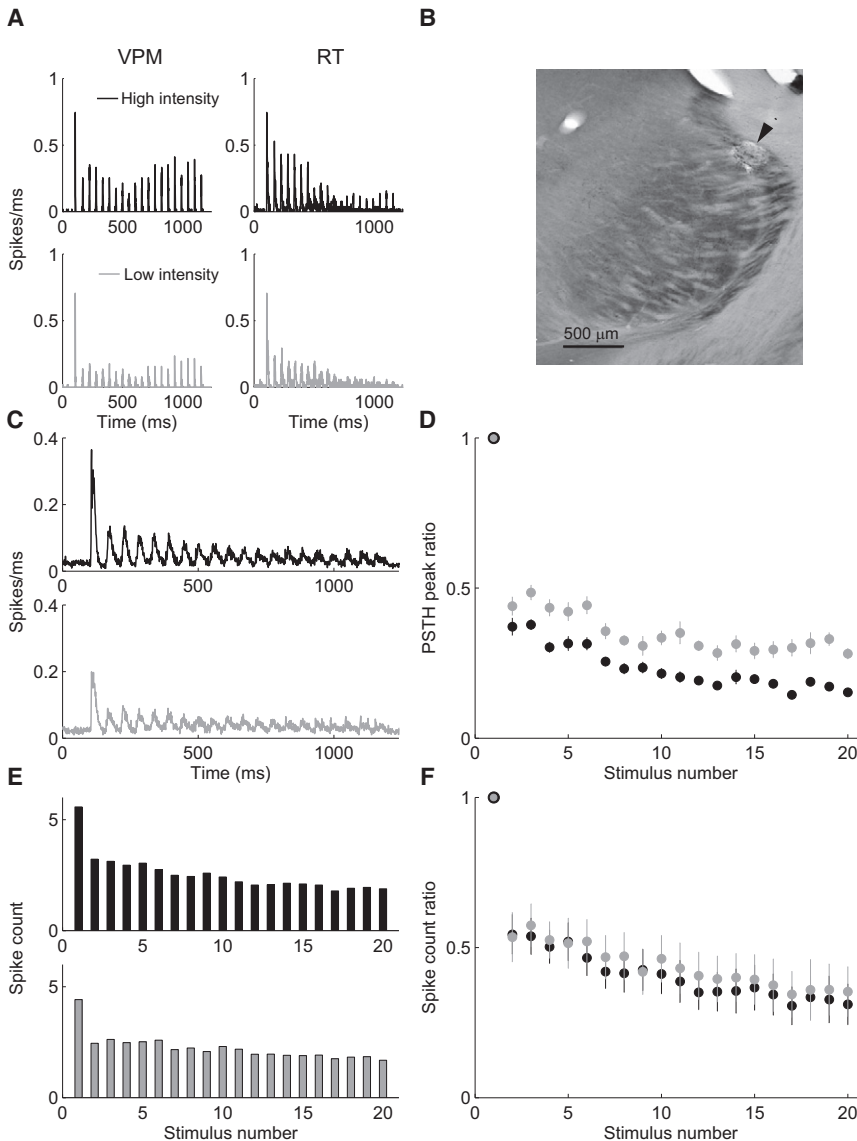


**Figure 5. Adaptation in the RT Is Less Dependent on Stimulation Intensity Compared to the VPM**

(A) Example PSTH of a paired whisker-aligned simultaneous recording of a VPM neuron (left) and RT multiunit activity (right) for both stimulus conditions. During stimulation, the VPM neuron exhibits significant recovery after the tenth stimuli, more so than RT activity.

(B) Lesions (marked by arrowhead) were used to verify that the location of the tip of the recording electrode was in the RT.

(C) RT population (n = 11) PSTH of multiunit activity in response to repetitive whisker stimulation at 18 Hz to both stimulus conditions.

(D) RT average PSTH peak response adaptation ratio is plotted against stimulus number (bars represent SEM). Actual PSTH peak values are divided by the peak of the first response to produce the ratio.

(E) Number of spikes evoked per stimulus (55 ms bins), in RT multiunit recordings, is plotted against stimulus number, for both intensity conditions.

(F) RT population average spike count adaptation ratio is plotted against stimulus number (bars represent SEM). Actual spike counts are divided by the number of spikes evoked by the first stimulus to produce the ratio. RT responses to low-intensity stimuli adapt slightly less than responses to high-intensity stimuli, opposite to what we observed in cortex and VPM.

faster when we increased stimulus intensity, similar to spiking adaptation (Figure 8B). This clearly does not agree with the “iceberg” model’s prediction and therefore implies that additional brainstem mechanisms are involved in generating the pattern of adaptation that we report in this study.

## DISCUSSION

We show that sensory responses to high-intensity repetitive whisker stimuli adapt less than responses to weaker stimuli. Our data suggest that this result cannot be explained by short-term synaptic depression alone, and we conclude that additional mechanisms are involved in sensory adaptation in the whisker to barrel pathway *in vivo*. We further demonstrate that this unexpected adaptation behavior affects cortical and thalamic response and may contribute to disambiguate sensory

responses to stimuli of different intensities during and after adaptation. Finally, we demonstrate that this differential gating of stimulus intensity occurs sub-thalamically in the brainstem.

## Adaptation to Repetitive Whisker Stimulation

The degree to which cortical and thalamic responses adapt differs substantially across various studies. Several studies of cortical layer 4 neurons reported pronounced adaptation at frequencies below 10 Hz (Castro-Alamancos, 2004; Chung et al., 2002; Gabernet et al., 2005) while in other studies adaptation was much less pronounced (Brecht and Sakmann, 2002; Ego-Stengel et al., 2005; Higley and Contreras, 2006; Khatri et al., 2004). Because neuronal responses along the lemniscal pathway are highly sensitive to the velocity of whisker deflection (Arabzadeh et al., 2003, 2005; Pinto et al., 2000) it is possible that in addition to other factors, such as anesthetics, differences in the degree of adaptation across studies are related to the intensity of whisker stimulation. More pronounced adaptation to weak whisker stimulation, as we show in this study, is consistent with single-unit recordings of thalamic cells in lightly narcotized rats (Temereanca et al., 2008). Our study extends this finding by showing that this behavior is further observed in the cortex and that it originates in the brainstem.

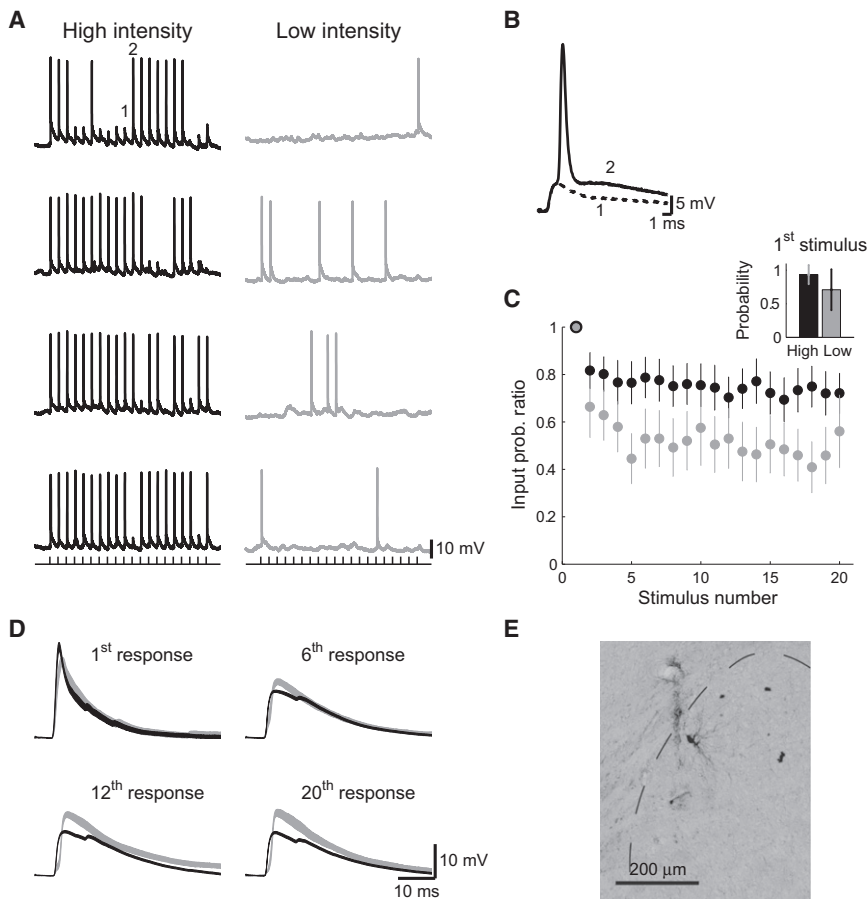


**Figure 6. Intracellular Recordings of VPM Neurons Reveal that Intensity-Dependent Adaptation Originates in the Brainstem**

(A) Example intracellular traces of a VPM neuron responding to an 18 Hz stimulus train. Stimulus times are depicted below the bottom traces. Large EPSPs evoked by stimulation are clearly observed. Failures to evoke spikes in the weak stimulus condition result from a complete absence of fast-rising synaptic input.

(B) Blow up of the EPSP (dashed line, 1) and spike (solid line, 2) indicated by numbers above the top left trace in (A). Traces are aligned to stimulus onset.

(C) The average probability of synaptic input (either fast-rising EPSP or spike) adaptation ratio is plotted against stimulus number. Fast-rising synaptic input is considered to be brainstem input, and therefore these EPSPs reflect brainstem firing activity. Actual probabilities are divided by the probability of synaptic input in response to the first stimulus to produce the ratio (bars represent SEM). (Inset) Probability of observing synaptic input in response to the first stimulus in the train, for both intensity conditions. Error bars represent STD. As in VPM and cortex, adaptation (measured by scaled probability) to low-intensity stimuli is greater than in the high-intensity condition.

(D) Example of average EPSP (only trials in which an EPSP was detected were averaged) recorded in a VPM neuron with spikes blocked using QX-314 (Cell-2 in main text). EPSPs evoked by low-intensity stimuli become significantly greater, compared to those evoked by high-intensity stimuli, toward the latter stimuli in the train, suggesting that synaptic failures are not a result of synaptic depression. Line width corresponds to mean  $\pm$  1 SEM.

(E) Reconstruction of the cell presented in (D). Dashed line represents VPM border.

**Synaptic Depression in Early Sensory Processing**

Several studies have shown that synaptic depression plays an important role in sensory adaptation in the whisker to barrel pathway (Beierlein and Connors, 2002; Castro-Alamancos, 2002b; Chung et al., 2002; Deschênes et al., 2003; Gabernet et al., 2005; Gil et al., 1997, 1999; Katz et al., 2006). Three synaptic stages cumulatively contribute to adaptation of layer 4 cortical neurons. Little is known about the properties of the trigemino-principalis synapse; however, it has been shown to reliably transmit stimuli at stimulation frequencies much greater than the one used in this study (18 Hz) (Deschênes et al., 2003). Additional adaptation in the thalamus may arise from short-term synaptic depression of the trigemino-thalamic synapse (Castro-Alamancos, 2002b; Deschênes et al., 2003). The degree of adaptation in thalamic cells (Figure 3D) was similar to that of the input probability to these cells (Figure 6C), suggesting that intrinsic thalamic mechanisms do not contribute to lemniscal adaptation to repetitive stimulation (Landisman and Connors, 2007). Adaptation in cortical cells that receive direct thalamic input (Figure 1) was substantially greater compared to the thalamus (Figure 2), in agreement with current views sug-

gesting that short-term depression of the thalamo-cortical synapse plays a significant role in cortical adaptation in vivo (Chung et al., 2002; Katz et al., 2006) and in vitro (Beierlein and Connors, 2002; Gabernet et al., 2005; Gil et al., 1997, 1999).

Notably, synaptic transmission may actually increase adaptation even without synaptic depression at a given synapse, due to the spiking threshold (“iceberg effect”). The nonlinearity of the spiking mechanism at earlier stages may itself increase the firing adaptation at later stages without additional synaptic plasticity mechanisms. In particular we find that neurons of the trigeminal ganglion show little response adaptation (Figure 2, see also Fraser et al., 2006), which may be enhanced at the following stages.

**Locating the Origin of Intensity-Dependent Adaptation**

Our recordings of TG, VPM, as well as PrV neurons verified that increasing stimulus intensity results in higher firing rates and a greater probability of spike generation, in agreement with previous reports (Shoykhet et al., 2000; Wilent and Contreras, 2004). The combination of higher spiking probabilities and synaptic depression is at the basis of our initial assumption

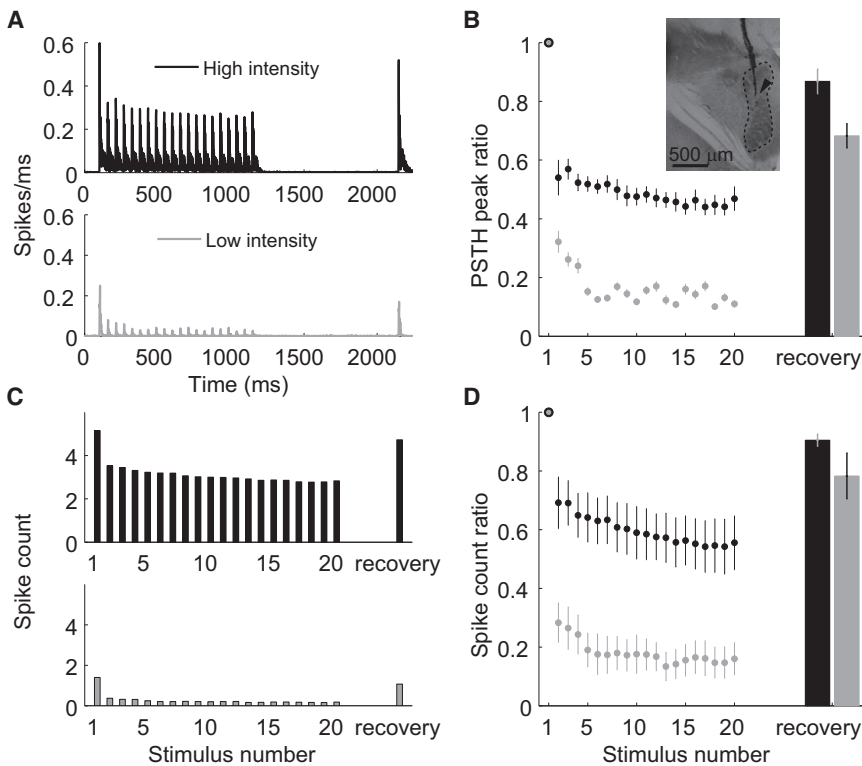


**Figure 7. PrV Recordings Provide Further Evidence that Intensity-Dependent Adaptation Originates in the Brainstem**

(A) PrV population ( $n = 11$ ) PSTH of responses to repetitive whisker stimulation at 18 Hz (20 stimuli) and a recovery response occurring 1 s after the end of the train, for both stimulus conditions.

(B) Average PSTH peak response adaptation ratio is plotted against stimulus number (error bars represent SEM). Actual PSTH peak values are divided by the peak of the first response to produce the ratio. Bar represents the recovery ratio (recovery response divided by the first response). (Inset) Brainstem slice showing electrode track (marked by arrowhead) through the PrV (dashed outline).

(C) Population average of the number of spikes evoked per stimulus (55 ms bins) is plotted against stimulus number, for both intensity conditions (rightmost bar corresponds to recovery response, 1 s after the end of the train).

(D) Average spike count adaptation ratio is plotted against stimulus number (error bars represent SEM). Actual spike counts are divided by the number of spikes evoked by the first stimulus to produce the ratio. Bar represents the recovery ratio (recovery response divided by the first response). PrV neurons adapt less and recover faster in response to high-intensity stimuli.

that responses to high-intensity stimuli should depress more than to weaker stimuli, since higher firing probability will result in higher effective frequency of stimulation (more stimuli will successfully evoke a spike) and in turn will cause greater synaptic depression. We showed, in contrast to this expected pattern of adaptation, that stronger stimulation entails less adaptation and that this behavior originates in the brainstem. To this end we recorded intracellularly in the VPM and extracellularly in the brainstem and pinpointed the location of the adaptation pattern to the brainstem PrV nucleus.

Although many PrV neurons project to VPM, other PrV neurons project to other brain regions, including the POm, Zona Incerta, and Superior Colliculus, among others (Veinante and Deschênes, 1999). Moreover, the PrV contains nonprojecting interneurons (Jacquin et al., 1990; Lo et al., 1999). Hence, recording the firing pattern of PrV neurons does not necessarily reveal the adaptation pattern received as input by VPM neurons. Whisker stimulation often evokes all-or-none large unitary EPSPs in VPM neurons, which reflect the firing of few fibers arriving from the PrV (Castro-Alamancos, 2002b; Deschênes et al., 2003). Hence, intracellular recordings allowed us to probe the probability of brainstem inputs to VPM cells. Our conclusions drawn from the intracellular recordings of VPM neurons were confirmed by extracellular recordings of PrV neurons, indicating that brainstem activity already exhibits intensity-dependent adaptation, in which responses to low-intensity stimuli adapt profoundly more than to stronger stimulation. Hence, brainstem provides a sufficient explanation for the unexpected intensity-dependent adaptation that we observed in the thalamus and cortex.

### Possible Mechanisms of Sensory Adaptation in the Brainstem

Our results indicate that TG neurons barely adapt and do so in an intensity-independent manner. On the other hand, PrV neurons adapt less and recover faster when driven by high-intensity stimuli. Since subcortical adaptation is thought to be governed by short-term synaptic depression, and synaptic depression models predict more adaptation when stimulation intensity is increased (opposite to what we observed), these results seem contradictory. How can these two observations (TG and PrV) be reconciled when they are only separated by a single synapse? Several alternative mechanisms may contribute to explain our findings:

- (1) Adaptation resulting from an “iceberg effect”—Inputs adapt as expected from short-term synaptic depression but the transformation into spikes flips the adaptation pattern. Consequently, despite the more profound synaptic depression caused by stronger stimulation, synaptic potentials are large enough to evoke firing during the stimulus train. On the other hand, synaptic inputs adapt very little during weak stimulation, however because the initial response is already close to threshold, the adapted responses barely cross the threshold, leading to greater spiking adaptation.

Though, such a situation is theoretically possible for a feed-forward model in which short term depression governs adaptation, as we observed by fitting the experimental adaptation phase with such a model, two main

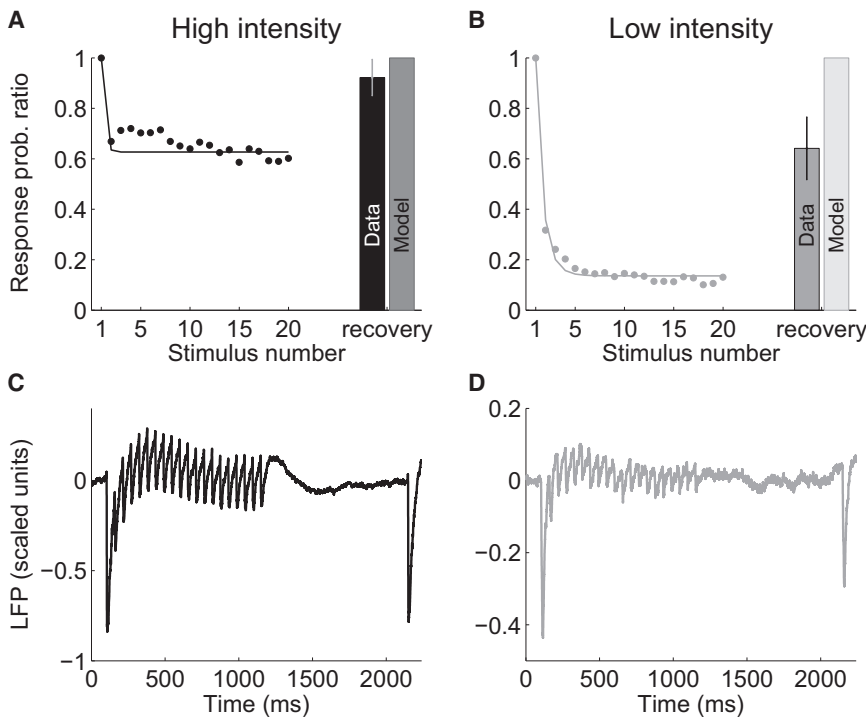


**Figure 8. Modeling and LFP Data Provide Evidence Against the “Iceberg Effect” as the Source for the Observed Adaptation Patterns**

(A) A simple model with synaptic depression and a nonlinear threshold (line) was fit to the brainstem PSTH peak data (dots) recorded during high-intensity stimulation (error bars represent SEM; see Supplemental Experimental Procedures for model details).

(B) Same as (A) but for weak stimulation. The model provides a good fit to the 20 responses to the high-frequency train but fails to predict the response to the recovery stimulus 1 s later (left bar, data; right bar, model). The recovery time constant attained from the fit was 50 ms, which results in complete recovery for both stimulus conditions. The only model parameter varied between the two stimulus conditions was the presynaptic firing probability.

(C) Population ( $n = 11$ ) average LFP evoked by high-intensity stimulation for the PrV (recorded simultaneously with the spikes that are presented in (A)).

(D) Same as (C) but for weak stimulation. Data from each neuron were normalized by the negative peak of the first response to the high-intensity stimulus before averaging (because across the population responses peaked at slightly different times, the average peak in C is smaller than 1 in

absolute value). While the “iceberg effect” predicts less adaptation to weak stimulation, the LFP measurements, as for spikes, also seem to adapt less and recover faster in the high-intensity condition, providing further evidence against the model of synaptic depression followed by a threshold.

findings strongly dismiss this possibility. First, our simulations (Figure 8) in which firing adaptation results from feed-forward short-term synaptic depression and a threshold failed to reproduce both the intensity-dependent adaptation and the slow recovery from weak repetitive stimulation. Second, LFPs recorded simultaneously with single and multiunits in the brainstem showed similar intensity-dependent adaptation and recovery as for the firing. Because LFP most likely reflects synaptic inputs (see Figure S3B for details), our data indicate that synaptic inputs adapt similarly to the firing pattern of the cells, and therefore the “iceberg effect” is not likely to be the source for the greater adaptation for weak stimulation.

- (2) Interplay between synaptic depression and synaptic facilitation of feed-forward inputs to brainstem neurons—Because of the low firing response of trigeminal ganglion cells during weak stimulation, short-term synaptic depression may govern synaptic dynamics. However, increasing the strength of stimulation elevates the firing probability of ganglion cells, which may cause a shift in the dynamics toward facilitation (Tsodyks et al., 1998). We note, however, that we are not aware of any report of synaptic facilitation in subcortical synapses along the lemniscal pathway. In addition, our brainstem LFP recordings show no evidence of facilitation.
- (3) A shift in the balance between excitation and inhibition during strong stimulation by a mechanism similar to the one reported in Heiss et al. (2008)—It is known that PrV

neurons receive substantial inhibitory inputs, mostly from sub-nucleus interparalis (Bellavance et al., 2010; Furuta et al., 2008; Lo et al., 1999). Accordingly, stronger stimulation may cause a substantial shift in the balance toward excitation, due to synaptic depression of inhibitory inputs.

- (4) Diverse populations of TG neurons—It is possible that PrV neurons receive inputs from a different population of TG neurons that we did not encounter in our experiments and possess adaptation properties qualitatively different than those displayed by the neurons we recorded.
- (5) Cortical feedback to PrV—The brainstem trigeminal complex receives substantial feedback from both the primary and secondary somatosensory cortices (Furuta et al., 2008). Such inputs may enhance the response to stronger stimulation due to the larger initial response during train stimulation.
- (6) Release-independent depression and activity-dependent recovery in afferent synapses—Synaptic depression behavior strikingly reminiscent of our findings was previously reported in paired recordings of cortical neurons in brain slices (Fuhrmann et al., 2004). This in vitro study reports that synapses displayed a reduction in response after stimulation, even in the absence of any observed synaptic release (release-independent depression), and furthermore, recovery from depression was actually enhanced when the synapse was activated more vigorously (activity-dependent recovery). Although the

underlying physiological mechanisms responsible for these phenomena have not yet been revealed, this behavior may fully explain our results.

While option (1) and (2) are unlikely given our experimental data, additional experiments both *in vivo* and *in vitro* are required to examine the other possibilities.

### Brainstem Adaptation and Coding of Sensory Stimulation

Assuming that adaptation is governed mainly by short-term synaptic depression, the response to high-intensity stimuli could possibly attenuate during this process to a level below that which is evoked by much weaker stimulation (see Figure 1B). This may greatly diminish the ability to discriminate stimulus intensities during adaptation. Given the above result, our study delineates how ambiguity may be prevented by brainstem processing. Because brainstem adaptation is much less pronounced for high-intensity stimulation, adaptation at downstream stages due to short-term synaptic depression may not be sufficient to cause ambiguity when the response is compared to those evoked by much weaker inputs. A similar process may also be involved in reducing the adaptation to strong stimulation and preventing intersection of adaptation response curves obtained at different intensities in the secondary somatosensory cortex of awake monkey (see Figure 1 of Ray et al., 2008).

Although the above conclusions may not hold for all possible stimuli, our data suggests this is the case for the higher frequency range of whisking behavior, as both thalamic and cortical response curves for different intensities do not intersect (Figures 1G and 3B, note that we refer to the nonscaled, absolute values). Similar results were observed when we applied different stimulation frequencies of 10 and 33 Hz, indicating that our results are relevant for a wide range of stimuli. Furthermore, as previously mentioned, the low-intensity stimulus varied across recordings; this suggests that our results are not limited to specific intensities, but rather to the relation between stimulus intensities (low versus high). We note, however, that the average low-intensity stimulation strength was similar across recording sites, supporting our view that the source of the reported behavior is common to all regions studied and originates in the brainstem (see Figure S1 and Table S1 for details).

In summary, we propose that the pattern of adaptation that we described at early stages of sensory processing may act to counterbalance the effects of short-term synaptic depression during sustained stimulation and filter out low-intensity noise, while increasing the duration and impact of persistent strong and perhaps relevant sensory inputs that otherwise would depress quickly.

## EXPERIMENTAL PROCEDURES

### Animal Preparation

Animal surgeries and *in vivo* recordings were performed as previously described (Katz et al., 2006). Briefly, recordings were made from young adult Wistar rats (4–8 weeks old,  $n = 5$  VPM units were recorded in adult Sprague-Dawley rats, with no qualitative differences in adaptation pattern). After initial anesthesia with ketamine (100 mg/kg) and xylezene (10%), a tracheotomy was made following local subcutaneous injection of lidocaine. Rats were

mounted in a stereotaxic device and respiration with a mixture of halothane (0.5%–1.5%) and oxygen-enriched air. The levels of end-tidal  $\text{CO}_2$  and heart rate (250–450 beats/min) were monitored throughout the experiment. Body temperature was kept at 37°C using a heating blanket and rectal thermometer. All surgical and experimental procedures were conducted in accordance with the regulations of the Weizmann Institute Animal Care and Use Committee.

### Cortical Patch Recordings

A craniotomy (0.5–1 mm in diameter) was made above the barrel cortex (centered 2.2 mm caudal and 5 mm lateral to bregma) and a portion of the dura mater was carefully removed. Whole-cell patch recordings were performed as previously described (Katz et al., 2006). Briefly, borosilicate micropipettes were pulled to produce electrodes with a resistance of 4–6 M $\Omega$ , and filled with an intracellular solution containing (in mM) 136 K-gluconate, 10 KCl, 5 NaCl, 10 HEPES, 1 MgATP, 0.3 NaGTP, and 10 phosphocreatine (310 mOsm). For histological identification of the recorded cells, 0.4% biocytin was added to the solution, and QX-314 (2 mM) was added to prevent action potentials. Intracellular signals were acquired using an Axoclamp-2B amplifier (Molecular Devices) and low pass filtered at 3 kHz before being digitized at 15 kHz.

### Thalamic Recordings

The craniotomy was centered 3 mm caudal, 3 mm lateral to bregma. Extracellular recordings were obtained at depths of 4.7–5.2 mm (vertical penetrations) using high-impedance (20–40 M $\Omega$ ) borosilicate micropipettes filled with standard ACSF. Extracellular signals were amplified using an Axoclamp-2B amplifier, band-pass filtered at 300 Hz to 5 kHz using a Cornerstone EX4-400 amplifier (Dagan Corp.) and digitized at 25 kHz. Intracellular recordings were performed using sharp electrodes filled with 2 M K-acetate with a resistance of 60–100 M $\Omega$ . Pipettes also contained biocytin (2%) and a subset of cells ( $n = 3$ ) were recorded with QX-314 (20 mM) in the solution as well. In some cells a hyperpolarizing current (<1.5 nA) was used in order to prevent excessive spiking.

### Reticular Thalamic Nucleus Recordings

Craniotomy was centered at 2.7 mm caudal, 3.5 mm lateral to bregma. Recording depths were 4.5–4.7 mm. Multiunit activity was recorded using Tungsten electrodes (0.5–1 M $\Omega$ ; Alpha Omega Engineering), amplified by MCP plus 8 (Alpha Omega Engineering) and digitized at 25 kHz. For paired RT-VPM recordings, an electrode was advanced at a 20° latero-medial angle from a point of contact of 2.7 mm caudal, 5.6 mm lateral to bregma, and recording depths were approximately 4.2–4.4 mm. Recording locations were marked by electrolytic lesions.

### Trigeminal Ganglion Recordings

Craniotomy was centered at 1 mm caudal, 2 mm lateral to bregma. Recordings were obtained using Tungsten electrodes as described above, at depths of 9.8–11 mm.

### Brainstem PrV Recordings

Craniotomy was centered ~1–2 mm caudal to lambda, 2.9 mm lateral to the midline. Tungsten electrodes were inserted caudorostrally at an angle of 5°–10° relative to the horizontal plane in the anterior part of the cerebellum. Electrode tracks were reconstructed histologically to verify recording location. Simultaneous LFP signals were obtained by band-pass filtering at DC–300 Hz.

### Histology

Procedures were previously described in Katz et al. (2006). Briefly, the brain was sectioned at a plane midway between coronal and sagittal (45°) for cortical reconstructions, or coronally for brainstem and thalamic reconstructions. Barrels were identified by cytochrome oxidase staining, and cells were reconstructed by performing diaminobenzidine (DAB) staining. Cortical neurons which were located inside a barrel, or had dendrites inside a barrel and a response latency <8 ms were considered as receiving direct thalamic input. Recording sites in the RT were marked by electrolytic lesions (ten 1 s

injections of 1 mA electrode positive currents, 1 s pause between current injections) to verify recording locations in the RT (Paxinos and Watson, 1986). Recording sites in the brainstem were verified by locating the electrode tracks in the slices.

### Whisker Stimulation and Protocols

Whiskers were trimmed to a length of 10–20 mm. The primary whisker was inserted into a 2 mm plastic cone glued into a metal pipette attached to the piezoelectric wafer (T220-H4-203Y; Piezosystems) which was driven by a homemade controller. The displacement near the tip of the metal pipette was measured off-line using an optical displacement measuring system (optoNCDT 1605; Micro-Epsilon). A fast-rising voltage command was used to evoke a fast whisker deflection with a constant rise time of ~1 ms followed by a 20 ms ramp-down signal. Because of the fixed rise time, amplitude and speed of deflection grow together with the magnitude of the voltage command, following a quasilinear relationship. The stimulation velocity at the high-intensity condition was ~50 mm/s (~145  $\mu$ m displacement). For the weak stimulus condition, stimulation velocity was set such that it evoked a response with much lower probability than the high-intensity stimulus. The average velocity for weak stimulation for the different recording sites can be seen in Table S1. A train of 20 stimuli at 18 Hz (55 ms interstimulus interval) was applied at each trial. Intertrial intervals were 2.7–3 s. For recovery protocols, an additional stimulus was delivered 1, 2.3, or 5 s after the last (20<sup>th</sup>) stimulus in the train. Intertrial interval for recovery protocol was 10 s. Different frequencies were tested using a similar protocol but with 30/55/100 ms interstimulus intervals and a test stimulus delivered 1 s after the last stimulus of the train (intertrial interval was 5 s). For each recording two stimulus intensities were used; trials were pseudorandomized.

### Conductance Estimates

For conductance estimates, stimulation trains were delivered at three or four different holding currents ranging from –0.3 to 0.4 nA. All trials were pseudorandomized. We estimated changes in excitatory and inhibitory conductances as previously described (Heiss et al., 2008). Briefly, the average voltage at each time step (smoothed and subsampled at 5 kHz) and its derivative, were fit by the membrane potential equation:  $I = C(dV_t/dt) + G_r(V_t - E_r) + G_e(V_t - V_e) + G_i(V_t - V_i)$ , where  $I$  is a vector of the injected currents and  $C$  is the estimated capacitance of the cell. Voltage-dependent conductances not blocked by QX-314 were partially accounted for by calculating the resting conductance in the absence of stimulation ( $G_r$ ) as the leak conductance corresponding to each current step.

### Short-Term Synaptic Depression Model

Short-term synaptic depression was modeled following Tsodyks and Markram (1997), see Supplemental Experimental Procedures for details.

### SUPPLEMENTAL INFORMATION

Supplemental Information includes Supplemental Experimental Procedures, three figures, and one table and can be found with this article online at doi:10.1016/j.neuron.2010.03.032.

### ACKNOWLEDGMENTS

We would like to thank Marina Taran and Valerie Mazig for their help with the histological reconstructions and Prof. M. Tsodyks and Muna Jubran for their helpful comments on this work. This work was supported by Grant No 326/07 from the Israel Science Foundation and by the Minerva Foundation funded by the Federal German Ministry for Education and Research and the Israeli Ministry of Science and Technology. Support was provided also by the Henry S. and Anne Reich Research Fund for Mental Health, the Asher and Jeanette Alhadeff Research Award, and Sir Charles Clore fellowship.

Accepted: March 24, 2010

Published: April 28, 2010

### REFERENCES

- Adorján, P., Piepenbrock, C., and Obermayer, K. (1999). Contrast adaptation and infomax in visual cortical neurons. *Rev. Neurosci.* 10, 181–200.
- Andermann, M.L., and Moore, C.I. (2006). A somatotopic map of vibrissa motion direction within a barrel column. *Nat. Neurosci.* 9, 543–551.
- Arabzadeh, E., Petersen, R.S., and Diamond, M.E. (2003). Encoding of whisker vibration by rat barrel cortex neurons: implications for texture discrimination. *J. Neurosci.* 23, 9146–9154.
- Arabzadeh, E., Zorzin, E., and Diamond, M.E. (2005). Neuronal encoding of texture in the whisker sensory pathway. *PLoS Biol.* 3, e17.
- Arabzadeh, E., Panzeri, S., and Diamond, M.E. (2006). Deciphering the spike train of a sensory neuron: counts and temporal patterns in the rat whisker pathway. *J. Neurosci.* 26, 9216–9226.
- Barlow, H.B. (1990). A Theory about the Functional Role and Synaptic Mechanism of Visual After-Effects. In *Vision: Coding and Efficiency*, C. Blackmore, ed. (Cambridge: Cambridge University Press), pp. 363–375.
- Beierlein, M., and Connors, B.W. (2002). Short-term dynamics of thalamocortical and intracortical synapses onto layer 6 neurons in neocortex. *J. Neurophysiol.* 88, 1924–1932.
- Bellavance, M.-A., Demers, M., and Deschênes, M. (2010). Feedforward inhibition determines the angular tuning of vibrissal responses in the principal trigeminal nucleus. *J. Neurosci.* 30, 1057–1063.
- Berg, R.W., and Kleinfeld, D. (2003). Rhythmic whisking by rat: retraction as well as protraction of the vibrissae is under active muscular control. *J. Neurophysiol.* 89, 104–117.
- Brecht, M., and Sakmann, B. (2002). Dynamic representation of whisker deflection by synaptic potentials in spiny stellate and pyramidal cells in the barrels and septa of layer 4 rat somatosensory cortex. *J. Physiol.* 543, 49–70.
- Brenner, N., Bialek, W., and de Ruyter van Steveninck, R. (2000). Adaptive rescaling maximizes information transmission. *Neuron* 26, 695–702.
- Bruno, R.M., and Sakmann, B. (2006). Cortex is driven by weak but synchronously active thalamocortical synapses. *Science* 312, 1622–1627.
- Carandini, M., and Ferster, D. (1997). A tonic hyperpolarization underlying contrast adaptation in cat visual cortex. *Science* 276, 949–952.
- Carvalho, T.P., and Buonomano, D.V. (2009). Differential effects of excitatory and inhibitory plasticity on synaptically driven neuronal input-output functions. *Neuron* 61, 774–785.
- Castro-Alamancos, M.A. (2002a). Different temporal processing of sensory inputs in the rat thalamus during quiescent and information processing states in vivo. *J. Physiol.* 539, 567–578.
- Castro-Alamancos, M.A. (2002b). Properties of primary sensory (lemniscal) synapses in the ventrobasal thalamus and the relay of high-frequency sensory inputs. *J. Neurophysiol.* 87, 946–953.
- Castro-Alamancos, M.A. (2004). Absence of rapid sensory adaptation in neocortex during information processing states. *Neuron* 41, 455–464.
- Chance, F.S., Nelson, S.B., and Abbott, L.F. (1998). Synaptic depression and the temporal response characteristics of V1 cells. *J. Neurosci.* 18, 4785–4799.
- Chelaru, M.I., and Dragoi, V. (2008). Asymmetric synaptic depression in cortical networks. *Cereb. Cortex* 18, 771–788.
- Chung, S., Li, X., and Nelson, S.B. (2002). Short-term depression at thalamocortical synapses contributes to rapid adaptation of cortical sensory responses in vivo. *Neuron* 34, 437–446.
- Cotillon-Williams, N., Huetz, C., Hennevin, E., and Edeline, J.M. (2008). Tonic control of auditory thalamus frequency tuning by reticular thalamic neurons. *J. Neurophysiol.* 99, 1137–1151.
- Deschênes, M., Timofeeva, E., and Lavallée, P. (2003). The relay of high-frequency sensory signals in the Whisker-to-barreloid pathway. *J. Neurosci.* 23, 6778–6787.
- Díaz-Quesada, M., and Maravall, M. (2008). Intrinsic mechanisms for adaptive gain rescaling in barrel cortex. *J. Neurosci.* 28, 696–710.

- Dragoi, V., Sharma, J., Miller, E.K., and Sur, M. (2002). Dynamics of neuronal sensitivity in visual cortex and local feature discrimination. *Nat. Neurosci.* 5, 883–891.
- Ego-Stengel, V., Mello e Souza, T., Jacob, V., Shulz, D.E., and Shulz, D.E. (2005). Spatiotemporal characteristics of neuronal sensory integration in the barrel cortex of the rat. *J. Neurophysiol.* 93, 1450–1467.
- Fairhall, A.L., Lewen, G.D., Bialek, W., and de Ruyter Van Steveninck, R.R. (2001). Efficiency and ambiguity in an adaptive neural code. *Nature* 412, 787–792.
- Fraser, G., Hartings, J.A., and Simons, D.J. (2006). Adaptation of trigeminal ganglion cells to periodic whisker deflections. *Somatosens. Mot. Res.* 23, 111–118.
- Fuhrmann, G., Cowan, A., Segev, I., Tsodyks, M., and Stricker, C. (2004). Multiple mechanisms govern the dynamics of depression at neocortical synapses of young rats. *J. Physiol.* 557, 415–438.
- Furuta, T., Timofeeva, E., Nakamura, K., Okamoto-Furuta, K., Togo, M., Kaneko, T., and Deschênes, M. (2008). Inhibitory gating of vibrissal inputs in the brainstem. *J. Neurosci.* 28, 1789–1797.
- Gabernet, L., Jadhav, S.P., Feldman, D.E., Carandini, M., and Scanziani, M. (2005). Somatosensory integration controlled by dynamic thalamocortical feed-forward inhibition. *Neuron* 48, 315–327.
- Gil, Z., Connors, B.W., and Amitai, Y. (1997). Differential regulation of neocortical synapses by neuromodulators and activity. *Neuron* 19, 679–686.
- Gil, Z., Connors, B.W., and Amitai, Y. (1999). Efficacy of thalamocortical and intracortical synaptic connections: quanta, innervation, and reliability. *Neuron* 23, 385–397.
- Gottschaldt, K.M., and Vahle-Hinz, C. (1981). Merkel cell receptors: structure and transducer function. *Science* 214, 183–186.
- Hartings, J.A., Temereanca, S., and Simons, D.J. (2003). Processing of periodic whisker deflections by neurons in the ventroposterior medial and thalamic reticular nuclei. *J. Neurophysiol.* 90, 3087–3094.
- Heiss, J.E., Katz, Y., Ganmor, E., and Lampl, I. (2008). Shift in the balance between excitation and inhibition during sensory adaptation of S1 neurons. *J. Neurosci.* 28, 13320–13330.
- Higley, M.J., and Contreras, D. (2006). Balanced excitation and inhibition determine spike timing during frequency adaptation. *J. Neurosci.* 26, 448–457.
- Jacquin, M.F., Chiaia, N.L., Haring, J.H., and Rhoades, R.W. (1990). Intersubnuclear connections within the rat trigeminal brainstem complex. *Somatosens. Mot. Res.* 7, 399–420.
- Jones, L.M., Lee, S.H., Trageser, J.C., Simons, D.J., and Keller, A. (2004). Precise temporal responses in whisker trigeminal neurons. *J. Physiol.* 92, 665–668.
- Katz, Y., Heiss, J.E., and Lampl, I. (2006). Cross-whisker adaptation of neurons in the rat barrel cortex. *J. Neurosci.* 26, 13363–13372.
- Kerr, J.N., de Kock, C.P., Greenberg, D.S., Bruno, R.M., Sakmann, B., and Helmchen, F. (2007). Spatial organization of neuronal population responses in layer 2/3 of rat barrel cortex. *J. Neurosci.* 27, 13316–13328.
- Khatri, V., Hartings, J.A., and Simons, D.J. (2004). Adaptation in thalamic barrel and cortical barrel neurons to periodic whisker deflections varying in frequency and velocity. *J. Neurophysiol.* 92, 3244–3254.
- Kohn, A. (2007). Visual adaptation: physiology, mechanisms, and functional benefits. *J. Neurophysiol.* 97, 3155–3164.
- Landisman, C.E., and Connors, B.W. (2007). VPM and PoM nuclei of the rat somatosensory thalamus: intrinsic neuronal properties and corticothalamic feedback. *Cereb. Cortex* 17, 2853–2865.
- Lo, F.-S., Guido, W., and Erzurumlu, R.S. (1999). Electrophysiological properties and synaptic responses of cells in the trigeminal principal sensory nucleus of postnatal rats. *J. Neurophysiol.* 82, 2765–2775.
- Lundstrom, B.N., Higgs, M.H., Spain, W.J., and Fairhall, A.L. (2008). Fractional differentiation by neocortical pyramidal neurons. *Nat. Neurosci.* 11, 1335–1342.
- Maravall, M., Petersen, R.S., Fairhall, A.L., Arabzadeh, E., and Diamond, M.E. (2007). Shifts in coding properties and maintenance of information transmission during adaptation in barrel cortex. *PLoS Biol.* 5, e19.
- Moore, C.I., and Nelson, S.B. (1998). Spatio-temporal subthreshold receptive fields in the vibrissa representation of rat primary somatosensory cortex. *J. Neurophysiol.* 80, 2882–2892.
- Müller, J.R., Metha, A.B., Krauskopf, J., and Lennie, P. (1999). Rapid adaptation in visual cortex to the structure of images. *Science* 285, 1405–1408.
- Paxinos, G., and Watson, C. (1986). *The Rat Brain in Stereotaxic Coordinates* (New York: Academic Press).
- Petersen, C.C. (2003). The barrel cortex—integrating molecular, cellular and systems physiology. *Pflügers Arch.* 447, 126–134.
- Pierret, T., Lavallée, P., and Deschênes, M. (2000). Parallel streams for the relay of vibrissal information through thalamic barreloids. *J. Neurosci.* 20, 7455–7462.
- Pinault, D. (2004). The thalamic reticular nucleus: structure, function and concept. *Brain Res. Brain Res. Rev.* 46, 1–31.
- Pinto, D.J., Brumberg, J.C., and Simons, D.J. (2000). Circuit dynamics and coding strategies in rodent somatosensory cortex. *J. Neurophysiol.* 83, 1158–1166.
- Ray, S., Hsiao, S.S., Crone, N.E., Franaszczuk, P.J., and Niebur, E. (2008). Effect of stimulus intensity on the spike-local field potential relationship in the secondary somatosensory cortex. *J. Neurosci.* 28, 7334–7343.
- Sanchez-Vives, M.V., Nowak, L.G., and McCormick, D.A. (2000a). Cellular mechanisms of long-lasting adaptation in visual cortical neurons in vitro. *J. Neurosci.* 20, 4286–4299.
- Sanchez-Vives, M.V., Nowak, L.G., and McCormick, D.A. (2000b). Membrane mechanisms underlying contrast adaptation in cat area 17 in vivo. *J. Neurosci.* 20, 4267–4285.
- Sarid, L., Bruno, R., Sakmann, B., Segev, I., and Feldmeyer, D. (2007). Modeling a layer 4-to-layer 2/3 module of a single column in rat neocortex: interweaving in vitro and in vivo experimental observations. *Proc. Natl. Acad. Sci. USA* 104, 16353–16358.
- Sharpee, T.O., Sugihara, H., Kurgansky, A.V., Rebrik, S.P., Stryker, M.P., and Miller, K.D. (2006). Adaptive filtering enhances information transmission in visual cortex. *Nature* 439, 936–942.
- Shosaku, A., Kayama, Y., Sumitomo, I., Sugitani, M., and Iwama, K. (1989). Analysis of recurrent inhibitory circuit in rat thalamus: neurophysiology of the thalamic reticular nucleus. *Prog. Neurobiol.* 32, 77–102.
- Shoykhet, M., Doherty, D., and Simons, D.J. (2000). Coding of deflection velocity and amplitude by whisker primary afferent neurons: implications for higher level processing. *Somatosens. Mot. Res.* 17, 171–180.
- Temereanca, S., Brown, E.N., and Simons, D.J. (2008). Rapid changes in thalamic firing synchrony during repetitive whisker stimulation. *J. Neurosci.* 28, 11153–11164.
- Tsodyks, M.V., and Markram, H. (1997). The neural code between neocortical pyramidal neurons depends on neurotransmitter release probability. *Proc. Natl. Acad. Sci. USA* 94, 719–723.
- Tsodyks, M., Pawelzik, K., and Markram, H. (1998). Neural networks with dynamic synapses. *Neural Comput.* 10, 821–835.
- Ulanovsky, N., Las, L., and Nelken, I. (2003). Processing of low-probability sounds by cortical neurons. *Nat. Neurosci.* 6, 391–398.
- Urbain, N., and Deschênes, M. (2007). A new thalamic pathway of vibrissal information modulated by the motor cortex. *J. Neurosci.* 27, 12407–12412.
- Veinante, P., and Deschênes, M. (1999). Single- and multi-whisker channels in the ascending projections from the principal trigeminal nucleus in the rat. *J. Neurosci.* 19, 5085–5095.
- Wainwright, M.J., Schwartz, O., and Simoncelli, E.P. (2002). *Natural Image Statistics and Divisive Normalization: Modeling Nonlinearities and Adaptation in Cortical Neurons* (Cambridge, MA: MIT Press).

- Wark, B., Lundstrom, B.N., and Fairhall, A. (2007). Sensory adaptation. *Curr. Opin. Neurobiol.* *17*, 423–429.
- Wehr, M., and Zador, A.M. (2005). Synaptic mechanisms of forward suppression in rat auditory cortex. *Neuron* *47*, 437–445.
- Wilent, W.B., and Contreras, D. (2004). Synaptic responses to whisker deflections in rat barrel cortex as a function of cortical layer and stimulus intensity. *J. Neurosci.* *24*, 3985–3998.
- Yu, C., Derdikman, D., Haidarliu, S., and Ahissar, E. (2006). Parallel thalamic pathways for whisking and touch signals in the rat. *PLoS Biol.* *4*, e124.
- Yu, X.J., Xu, X.X., Chen, X., He, S., and He, J. (2009). Slow recovery from excitation of thalamic reticular nucleus neurons. *J. Neurophysiol.* *101*, 980–987.
- Zucker, R.S., and Regehr, W.G. (2002). Short-term synaptic plasticity. *Annu. Rev. Physiol.* *64*, 355–405.